



Bridge's Overall Structural Scheme Analysis in High Seismic Risk Permafrost Regions

Zhihua Xiong ¹, Jianbing Chen ^{2*}, Chen Liu ¹, Jinping Li ², Wenwen Li ¹

¹ College of Water Resources and Architectural Engineering, Northwest A&F University, Yangling, 712100, China.

² CCCC First Highway Consultants Co. Ltd. Yanta, Xi'an, 710065, China.

Received 10 April 2022; Revised 23 June 2022; Accepted 27 June 2022; Published 01 July 2022

Abstract

The mechanism of pile-soil reaction in frozen ground is not clear at present, but it is obvious that the reduction of dead weight will be beneficial to the seismic resistance of bridges. In view of the limited bridge engineering practice in high seismic risk permafrost regions, the paper addressed the structural performance of the superstructure and its effect on piles in these special regions. Four superstructures with different dead weights were compared, and bored piles were designed. Numerical simulations were implemented to investigate the refreezing time of the bored pile foundation. The concrete pile cooled rapidly in the first two days. The refreezing times of the GFRP, prestressed concrete T-girder, integrated composite girder, and MVFT girder were 15d, 37d, 39d, and 179d, respectively. The refreezing time of a pile in the same soil layer is mainly affected by the pile's diameter, and it is significantly correlated to the square of the pile diameter. It reflects that the selection of bridge superstructures in the permafrost region is very important, which has been ignored in previous studies. The pile length and pile diameter of the lighter superstructure can be shorter and smaller to reduce the refreezing time and alleviate the thermal disturbance.

Keywords: Permafrost; High Seismic; Bridge; Scheme; Pile.

1. Introduction

Permafrost areas account for 22.4 percent of the land area of China, mainly distributed in the Qinghai-Tibet Plateau (QTP) and northeast China [1]. With the accelerating process of western development, Tibet and Qinghai Province have a great expectation of economic development in the Fourteenth Five-Year Plan. In addition, there are large areas affected by permafrost along "The Belt and Road Initiative" [2], along which massive infrastructure constructions are needed. In the Qinghai-Tibet railway, bridges account for about 23% of the total line [3]. The embankment is the main part of the route and there is a great deal of research work on its structural form and temperature characteristics [4]. However, settlement induced by the temperature of the embankment is larger than that of a bridge in the permafrost regions. The main problems for small and medium bridges in the Qinghai-Tibet Plateau include seismic risk and durability.

The Qinghai-Tibet Plateau is the most intensive seismic area in China [5], yet without a corresponding seismic specification for bridge design in the permafrost regions [6]. The interaction mechanism and the failure characteristics of pile-foundation and frozen soil systems in the permafrost regions under earthquakes are unclear [7]. Permafrost has degraded constantly [8, 9], which will directly lead to the decline of pile bearing capacity in permafrost regions [10]. The bored pile is the most common type of pile foundation in frozen regions [11]. The main factors determining pile bearing capacity include soil mass, water content, structural materials, surface roughness, and freezing temperature [12,

* Corresponding author: 57003307@qq.com

 <http://dx.doi.org/10.28991/CEJ-2022-08-07-01>



© 2022 by the authors. Licensee C.E.J, Tehran, Iran. This article is an open access article distributed under the terms and conditions of the Creative Commons Attribution (CC-BY) license (<http://creativecommons.org/licenses/by/4.0/>).

13]. Most of the bearing capacity of friction piles in frozen ground is provided by resistance to shear along the surface of the pile, frozen together with the soil [14]. Factors affecting the early thermal stability of bored pile foundations include hydration heat of concrete, mold entry temperature, hole-forming method, pile diameter, pile length, pile spacing, frozen soil geological conditions, etc. Among these factors, the hydration heat of concrete is the main factor [15]. The calculation and analysis of hydration heat have been investigated by Jia et al. [16]. Hou et al. discovered that the pile foundation's highest temperature occurred two days after the concrete was poured, 93 days after the concrete was poured, and the temperatures at various depths of the pile foundation plummeted below 0 °C [17]. To accelerate freezing, Chen [18] studied a quick-freezing system and verified its feasibility through field experiments. Shang et al. (2020) [19] proposed a two-phase closed thermosyphon (TPCT) and concrete piles to obtain a temperature control scheme with significant effect, and found the optimal TPCT length. Shang et al. (2018) [20] proposed a cold air refrigerant system to reduce refreezing time and the effect was evaluated. Combined with concrete maintenance and reduction of thermal disturbance of frozen soil, Yan & Yu [21] suggested that construction could be done with insulation on the outside of foundation piles to obtain a more uniform concrete temperature field, thus improving the concrete strength and reducing the disturbance of frozen soil. The construction period should be back frozen in the summer. Based on monitoring and simulation, Hou et al. [22] analyzed the thermal behavior of CIP group piles in the permafrost zone. These studies mainly focused on the rapid cooling of piles by artificial methods.

Due to the insufficient knowledge on prevention and mitigation of infrastructure disasters in high seismic risk permafrost regions, it is vital to investigate the bridge's structural scheme to guarantee its safety. On May 22, 2021, a 7.4-magnitude earthquake occurred in Maduo, Qinghai, causing a continuous multi-span girder to fall which included 19 spans on one line and 18 spans on the other line. The main reasons for the failure were a large structural response of prestressed concrete girder and shear damage of bearing [23]. The weight of the superstructure is the main factor of structure seismic response and will directly affect the design of pile diameter and length of the foundation. Therefore, the superstructure's type is a governing factor for the bridge in high seismic permafrost regions, and its scheme selection is the highlight of this research. The length and diameter of the pile are determined by the superstructure's dead weights, which will lead to a significant difference in refreezing time. However, the current research on pile refreezing does not take this into account. In this paper, the pile foundation design and refreezing simulation of different superstructure schemes have been carried out. The flowchart of the study is shown in Figure 1.

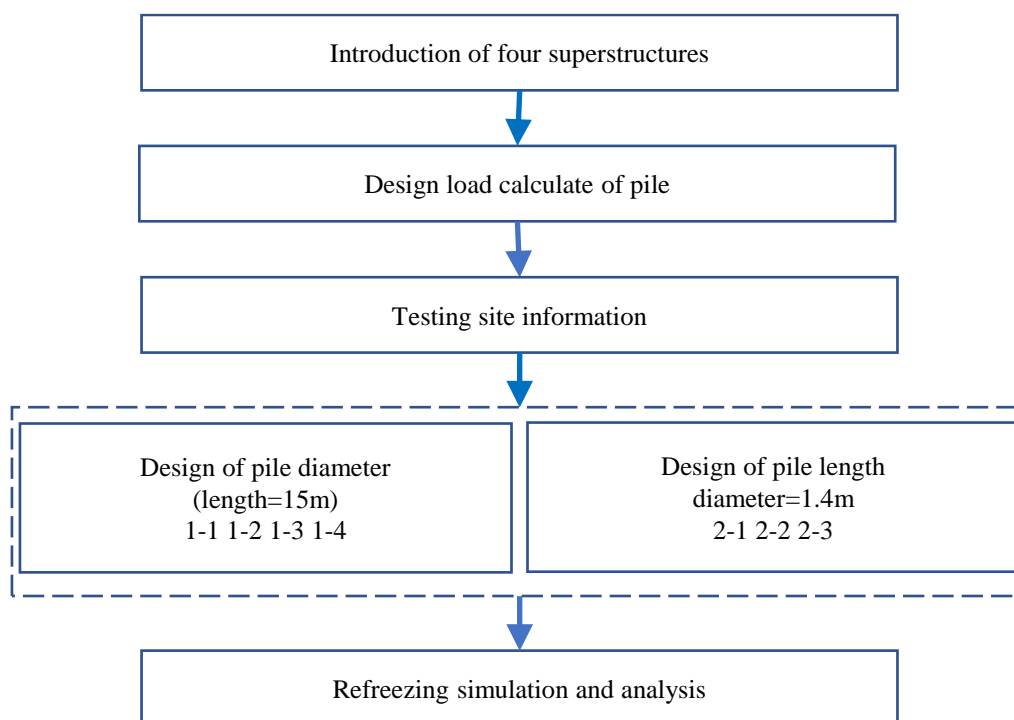


Figure 1. Flowchart of the study

2. Bridge Superstructure

The superstructure of the bridge determines the substructure and auxiliary structures. The dead weight of different superstructure schemes significantly affects the whole structural performance, especially in the high seismic risk permafrost regions. Four available superstructures have been involved and compared in the following contents. Ultimate limited state load combination has been used in the analysis model was listed in Table 1.

Table 1. Summary of superstructure parameters

| Bridge scheme | GFRP girder | MVFT girder | Integrated composite girder | P.C. T-girder |
|--|--------------|---------------|-----------------------------|---------------|
| Span (m) | 15 | 30 | 30 | 30 |
| Width (m) | 13 | 13 | 13 | 12.7 |
| Concrete (m^3) | 37.8 | 159 | 94.1 | 142.6 |
| Girder materials (kg) | 10260 (GFRP) | 65450 (Steel) | 74690 (Steel) | 50820 (Steel) |
| The weight of the upper structure (kN) | 991 | 4376 | 2365 | 3852 |
| Pile load (kN) | 684.25 | 2485.5 | 1480 | 2223.5 |

2.1. GFRP- Concrete Box Girder

Fiber reinforced polymer (FRP) has the advantages of light weight, high strength, corrosion resistance, and easy processing, etc. Its production processes include pultrusion, winding, hand paste, and molding [24]. In view of the FRP/Reinforced-concrete superstructure’s excellent structural performance [25], a glass fiber reinforced polymer (GFRP) concrete box girder was designed which was applicable to a span of 10~15m as shown in Figure 2. The material consumption of pultruded GFRP and concrete is listed in Table 1. The advantage of its light weight is easily observed.

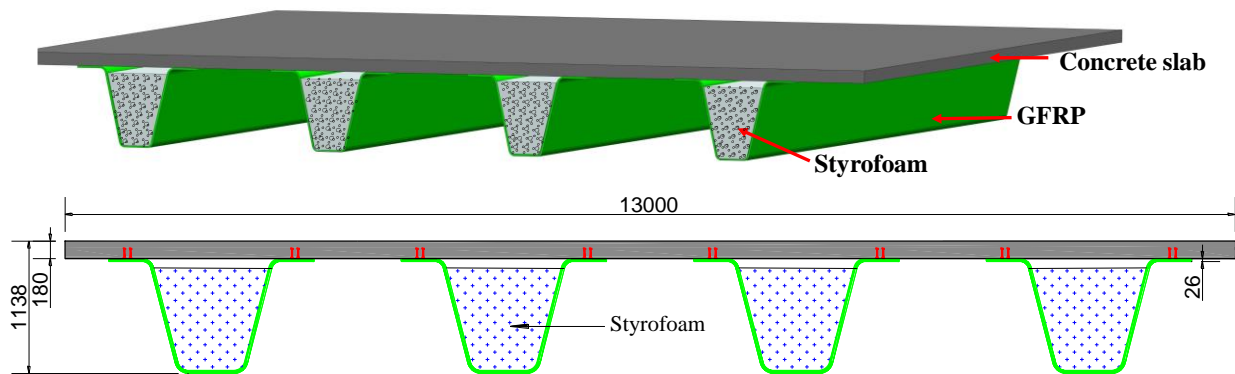


Figure 2. GFRP- Concrete box girder (mm)

2.2. MVFT Girder

The composite girder known as the Verbund-Fertigteile-Träger (VFT) was first designed in Germany and is now utilized in bridge construction throughout Europe [26]. In order to accelerate the construction speed, the author proposed the Modified Verbund-Fertigteile-Träger (MVFT) girder based on VFT girder in Figure 3, which was suitable for small and medium span bridges [27, 28]. In terms of MVFT girder, the concrete slabs and box girders were prefabricated in the factory and transported to the site for assembly and cast-in-place concrete. The material consumptions of steel and concrete are listed in Table 1.

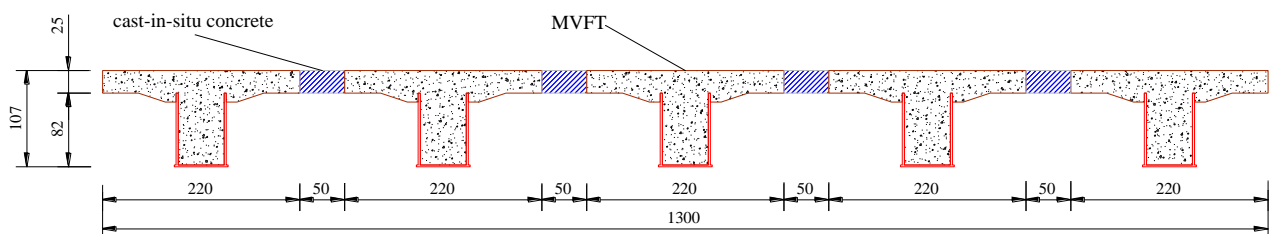
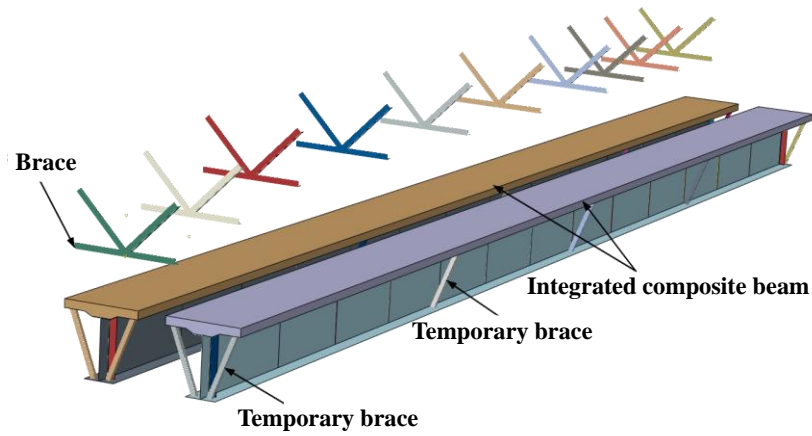


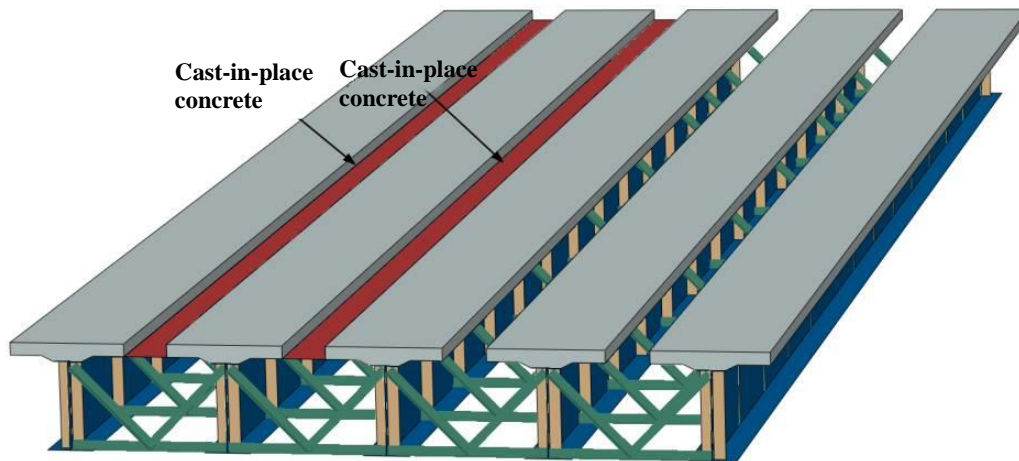
Figure 3. Section of MVFT girder (cm)

2.3. Integrated Composite Girder

The fatigue problem of the traditional orthotropic steel bridge deck is prominent in long-time service. However, the integrated composite girder which is shown in Figure 4 could eliminate this trouble, and it has advantages in both the weight and durability performance of the structure. Its weight is only 54% of the MVFT girder. The material consumption of an integrated composite girder is summarized in Table 1.



(a) 3D assembly of integrated composite girder



(b) Horizontal layout of bridge deck

Figure 4. Integrated composite girder [29]

2.4. Prestressed Concrete T-Girder

The prestressed Concrete T girder (P.C. T-girder) is widely used in highway construction in cold regions (Figure 5). Its weight is 163% of the integrated composite girder. The material consumption of P.C T-girder is listed in Table 1.

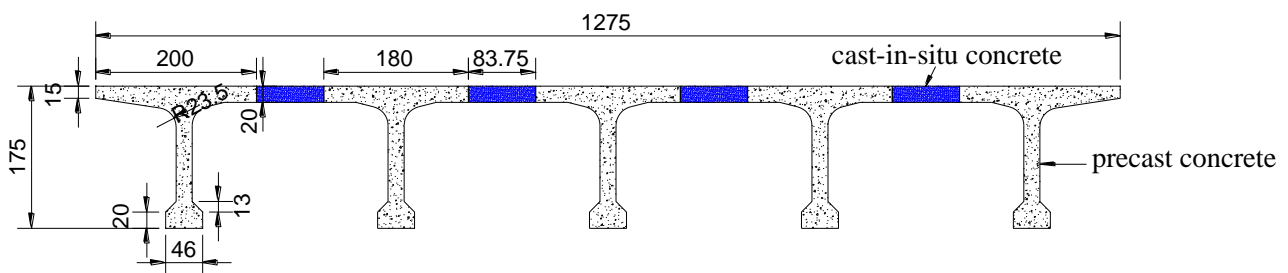


Figure 5. Diagram of P.C. T-girder mid-span cross section (cm)

As observed in Table 1, the composite structure can effectively reduce the dead weight and weaken the seismic response. The pile foundation will be designed according to Table 1, and then the refreezing simulation will be carried out.

3. Pile Foundation Design

3.1. Testing Site Information

The test site is located in Beiluhe Basin on the north slope of Fenghuo Mountain on the Tibetan Plateau, which is marked in Figure 6. The surface is flat and the vegetation is sparse. The shallow layer of the surface is mostly wind-sand

sediment, and there are hot melt lakes and ponds nearby. The altitude is 4618 m. The climate is cold and dry. The annual average temperature, precipitation, and evaporation of the site are -3.8°C , 290.9 mm, and 1316.9 mm, respectively. High-temperature unstable permafrost is widely distributed in Beiluhe regions. The permafrost table is generally between 1.5~3.0 m. The frozen soil is mainly consisted of clay and severely-weathered claystone as the drilling catalog of the cap in Figure 7 [30].

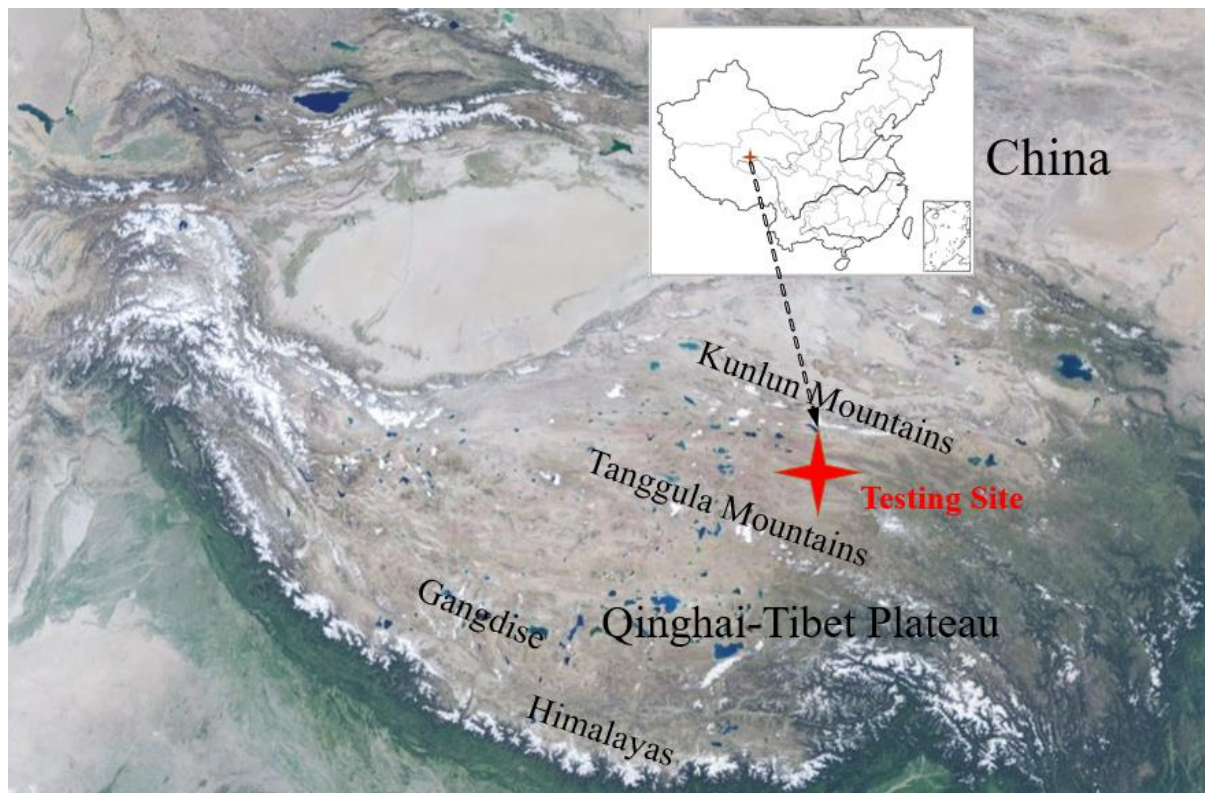


Figure 6. Testing site

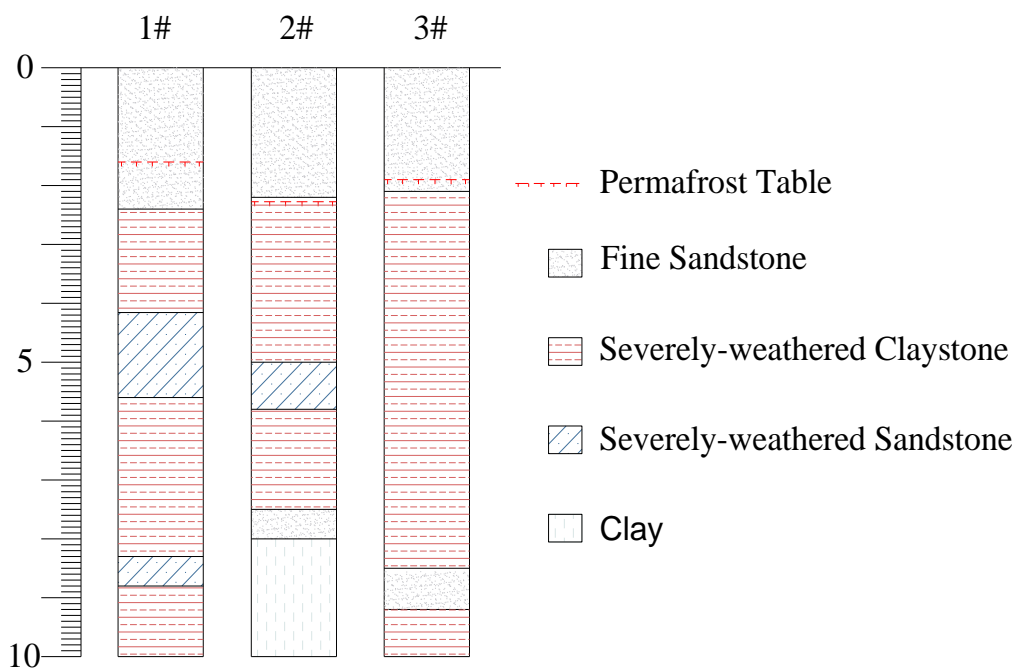


Figure 7. Drillhole information (m)

The following computed soil layers are shown in Figure 8 as a consequence of artificial modifications and forecasts due to the three boreholes' various findings and generalization considerations.

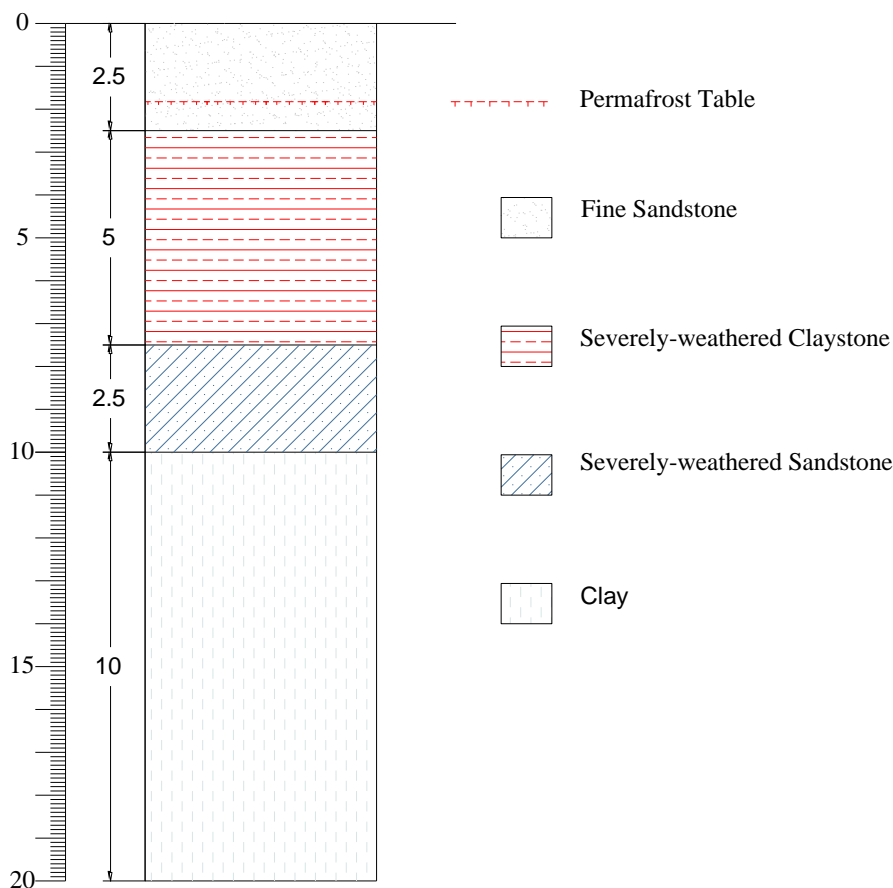


Figure 8. Schematic diagram of calculated soil layer (m)

Table 2. Material parameters of soil

| Soil group | Density (kg·m ⁻³) | Elastic modulus (MPa) | Freezing strength (kPa) | Carrying capacity (kPa) |
|-------------------------------------|-------------------------------|-----------------------|-------------------------|-------------------------|
| Fine Sandstone (-2°C) | 1920 | 16 | 70 | 300 |
| Severely-weathered Claystone (-4°C) | 2500 | 7 | 70 | 250 |
| Severely-weathered Sandstone (-2°C) | 2500 | 9 | 100 | 300 |
| Clay (-1°C) | 1800 | 5 | 60 | 400 |

3.2. Pile Foundation Design

Bored piles were used in the four superstructures schemes. According to Specifications for Design of Foundation of Highway Bridges and Culverts [31], the designed diameter of bored pile should be more than 0.8m. The upper layer of frozen soil is fine sand, which is not frost heaving soil. Hence, the pullout performance is ignored in the analysis. The bonding strength of melting sand soil is 30kPa. The ultimate bearing capacity of single pile can be calculated by the following expression:

$$R_a = \frac{1}{2} u \sum_{i=1}^n q_{ik} l_i + A_p q_r \tag{1}$$

where R_a is the axial compression bearing capacity of single pile; u is the perimeter of pile; n is the number of soil layers; l_i is the thickness of the soil; q_{ik} is the friction resistance corresponding to the various soil and pile side to l_i ; A_p is the section area of pile tip; q_r is the soil bearing capacity of pile tip.

The thermal disturbance range of concrete hydration heat on pile side increases in relation to the square of pile diameter, and the thermal disturbance range on pile bottom has a positive linear relationship with the pile length [32]. The temperature refreezing simulation of the following pile diameter and pile length was performed using the control variate approach. And the simulation scheme was shown in Table 3.

Table 3. Pile foundation design

| Scheme 1: length=15 m | | | | |
|--------------------------|-------------|-------------|-----------------------------|---------------|
| Bridge scheme | GFRP girder | MVFT girder | Integrated composite girder | P.C. T-girder |
| Group | 1-1 | 1-2 | 1-3 | 1-4 |
| Diameter (m) | 0.8 | 1.3 | 0.8 | 1.2 |
| Pile length (m) | 6.5 | 15 | 15 | 15 |
| Scheme 2: diameter=1.4 m | | | | |
| Bridge scheme | GFRP girder | MVFT girder | Integrated composite girder | P.C. T-girder |
| Group | | 2-1 | 2-2 | 2-3 |
| Diameter (m) | <i>NO.</i> | 1.4 | 1.4 | 1.4 |
| Pile length (m) | | 12 | 7.2 | 10.5 |

where, *No.* means no comparison for the span of GFRP girder is different to the other.

4. Refreezing Simulation of Pile Foundation

4.1. Modeling and Boundary Conditions

At present, there are two ways to study the temperature field of the bored piles in frozen regions: field experiments and numerical simulations. The thermal disturbance of frozen soil 2 m away from the pile has little influence, and the influence range is less than 4 times the pile diameter. The temperature of the soil layer around the pile will drop down to close to the natural in 200 days (d) [33, 34]. Therefore, a cylinder with a radius of 10 m and a depth of 20 m has been determined for modeling. Adiabatic boundary conditions were selected around the perimeter.

4.2. Heat of Hydration

Since the time required for refreezing was the only factor considered in the simulation, the exothermic analysis of hydration heat with time was not performed. For the sake of safety, the hydration heat of cement is considered a one-time release, and the final hydration heat release value of cement is 364 kJ/kg [35]. Assuming that the temperature of concrete is evenly distributed and the cement consumption per cubic meter is 415 kg, the absolute temperature rise of concrete is determined to be 65°C. Given that the mold temperature is 3°C, the initial concrete temperature is set at 68°C.

4.3. Initial Ground Temperature and Thermophysical Parameters

Soil thermal conductivity is affected by soil moisture, temperature, texture, and other factors [36]. The initial ground temperature was selected simply. The fine sand layer was set as -2°C, the strongly weathered mudstone layer was set as -4°C, the strongly weathered sandstone layer was set as -2°C, and the clay layer was set as -1°C. It is assumed that latent heat of phase transformation associated with the thawing of frozen soil is not considered.

Table 4. Thermophysical parameters of materials

| Materials | λ W/(m·°C) | C J/(kg·°C) |
|--------------------------------------|-----------------------|----------------|
| Fine Sandstone (-2 °C) | 1.92 | 1078 |
| Severely-weathered Claystone (-4 °C) | 2.4 | 788 |
| Severely-weathered Sandstone (-2 °C) | 1.82 | 800 |
| Clay (-1 °C) | 0.47 | 1188 |
| Concrete | 1.54 | 970 |

where, λ is Conductivity; C is Specific heat

4.4. Numerical Model and Results

The numerical model was created by ABAQUS, in which the linear hexahedral element of DC3D8 was implemented as shown in Figure 9.

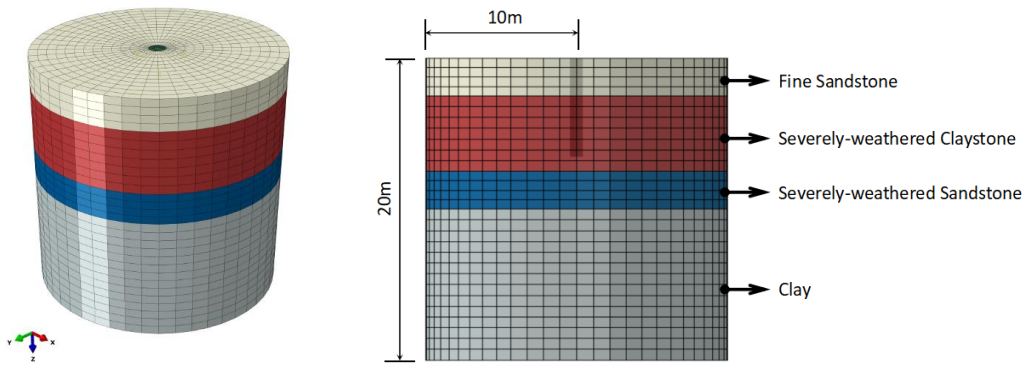
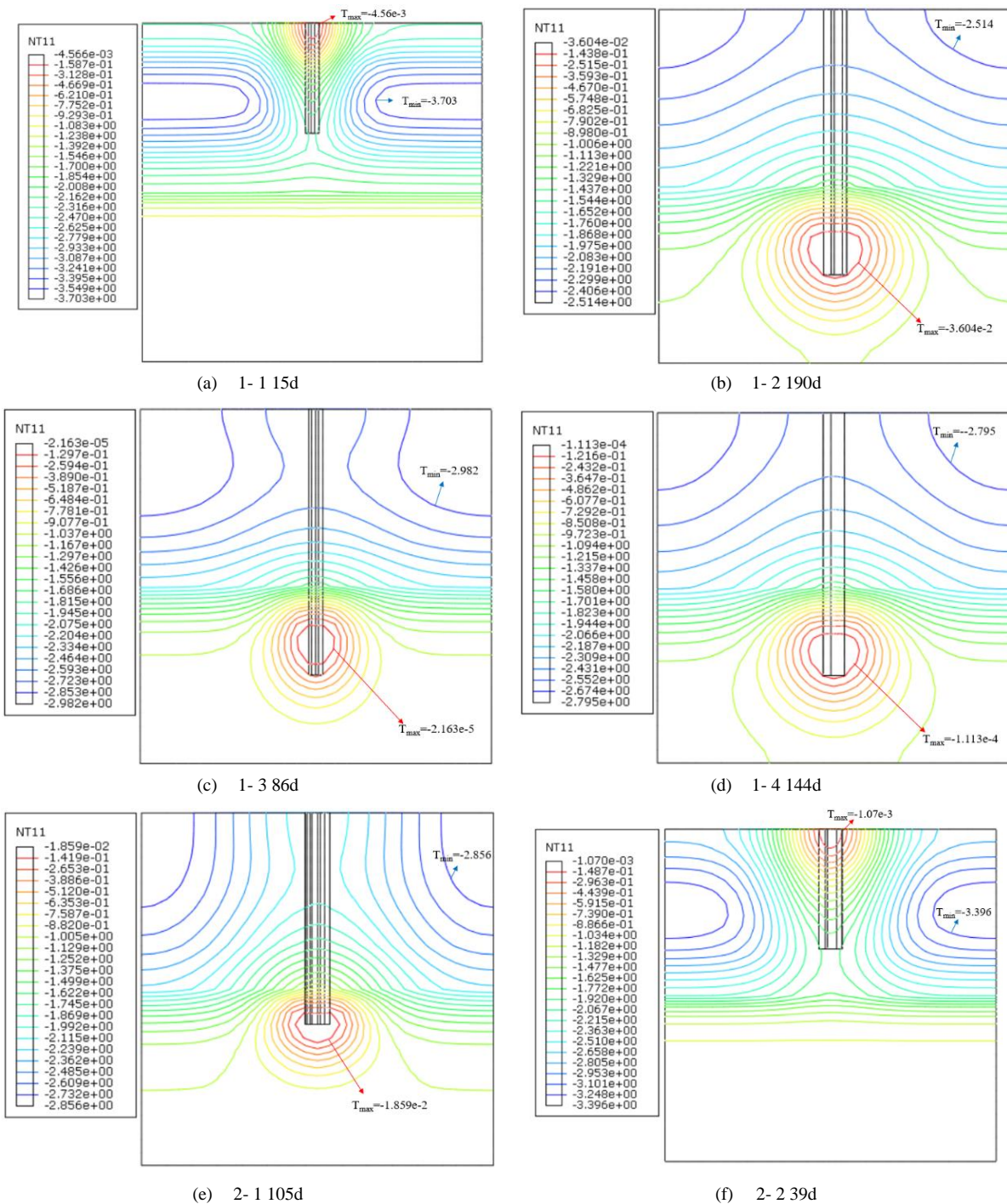


Figure 9. Layer and mesh of model

The simulation results of Table 3 are shown in Figure 10. The red contour line represents a higher temperature, and the blue contour line represents a lower temperature.



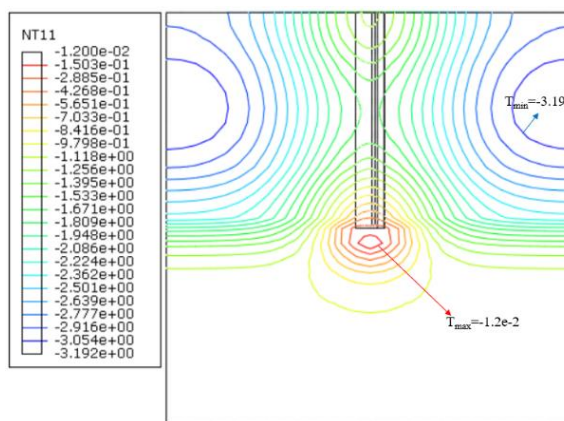


Figure 10. Pile refreezing temperature nephogram (d: day)

The time taken to reach the negative temperature is listed in Table 5.

Table 5. Total refreezing time of pile

| Group | 1-1 | 1-2 | 1-3 | 1-4 | 2-1 | 2-2 | 2-3 |
|-----------------------------------|-----|-----|-----|-----|-----|-----|------|
| Diameter (m) | 0.8 | 1.3 | 0.8 | 1.2 | 1.4 | 1.4 | 1.4 |
| Length (m) | 6.5 | 15 | 15 | 15 | 12 | 7.2 | 10.5 |
| Time to negative temperatures (d) | 15 | 190 | 86 | 144 | 105 | 39 | 52 |

The refreezing time of pile for different soil layers is listed in Table 6.

Table 6. Refreezing time of each soil layer

| Layer | Group | 1-1 | 1-2 | 1-3 | 1-4 | 2-1 | 2-2 | 2-3 |
|------------------------------|----------------|-----|------|-------|------|------|-----|-----|
| | Fine Sandstone | | 15d | 37d | 17d | 28d | 37d | 39d |
| Severely-weathered Claystone | | 8d | 29d | 8d | 20d | 27d | 24d | 28d |
| Severely-weathered Sandstone | | | 70d | 18.5d | 56d | 54d | | 43d |
| Clay | | | 190d | 86d | 144d | 105d | | 52d |

4.5. Discussion

From the analysis results of Figures 10-b, 10-c, 10-d, and 10-e, the longer the pile length is, the higher the temperature of the lower soil layer is, and the time required for the pile foundation to completely reduce to negative temperature is greatly increased. The difference in refreezing time of them is mainly caused by the pile diameter. The refreezing time at the center of the pile in the same soil layer is approximately proportional to the square of pile diameter, which corresponds to the heat change formula: $Q = m \cdot c \cdot \Delta T = \rho \cdot h \cdot \pi \cdot r^2 \cdot c \cdot \Delta T$. It can also be seen that the differences between the refreezing times of the same soil layer are not obvious when the pile diameter is similar as shown in Table 6, and the cooling rate is directly related to the soil temperature and thermal conductivity. It can also be found that the refreezing time is mainly consumed at the lower part of the pile which is in the frozen soil layer with lower thermal conductivity and higher temperature. The thermal conductivity of clay is close to 1/3 of that of concrete. The heat conduction of the pile foundation in this layer is slow, and the heat conducts upward along the pile, which increases the refreezing time of the pile foundation in a strong wind-blown sand stratum. As the initial temperature of the soil layer gradually warms up from top to bottom, the refreezing time increases significantly with the increase of pile depth.

Therefore, from the analysis of the same superstructure but with a different pile design, it can be found that reasonable optimization of pile diameter and length will be beneficial to decrease refreezing time. The concrete pile will be cooled rapidly in the first two days, usually to 3~4 °C, followed by more gradual cooling. Therefore, if the concrete pile can be artificially cooled effectively at a high temperature, it will greatly contribute to shortening the refreezing time and reducing the thermal disturbance of the pile to the surrounding soil.

5. Conclusions

- The refreezing times of the GFRP girder, integrated composite girder, and P.C. T-girder were 15d, 39d, and 52d respectively. Due to the weight of the MVFT girder, it took 179 days to completely refreeze, which was mainly controlled by the pile tip. Therefore, the lighter superstructure is preferred in cold regions since the pile diameter and length can be reduced to a certain degree, which will significantly reduce the refreezing time and make the thermal disturbance smaller. In the meantime, the composite superstructures are relatively lighter than prestressed concrete girders, which naturally lowers the bridge's structural damage risk during an earthquake.
- The refreezing time of a pile in the same soil layer is mainly affected by the pile's diameter, and it is significantly correlated to the square of the pile diameter. In particular, the time is around 16d and 38d for the fine sandstone layer when the diameter is 0.8 m and 1.4 m, respectively. Due to the large thermal conductivity of concrete, the heat conduction phenomenon along the pile is the main heat transfer pattern in the final phase of refreezing time.
- The pile diameter and length should be optimized under the condition of satisfying the structural and seismic requirements. The hydration heat of cement in concrete is mainly released in the early 3 days. It means that artificial cooling can greatly reduce the disturbance to soil and is beneficial for shortening the refreezing time. However, the thermal insulation measures for pre-curing concrete also need care in the later refreezing period. From both angles of refreezing time and dead weight, the composite superstructures are recommended.

6. Declarations

6.1. Author Contributions

Conceptualization, Z.X., and J.C.; methodology, Z.X.; software, C.L.; validation, Z.X., J.L. and W.L; formal analysis, C.L.; investigation, Z.X.; resources, J.C.; data curation, C.L.; writing—original draft preparation, W.L.; writing—review and editing, Z.X.; visualization, J.L.; supervision, J.C.; project administration, Z.X.; funding acquisition, Z.X. All authors have read and agreed to the published version of the manuscript.

6.2. Data Availability Statement

The data presented in this study are available in the article.

6.3. Funding

The authors appreciate the funding of State Key Laboratory of Road Engineering Safety and Health in Cold and High-altitude Regions (YGY2020KYPT-06).

6.4. Conflicts of Interest

The authors declare no conflict of interest.

7. References

- [1] Zhang, T. (2001). [Review of Geocryology in China, by Z. Youwu, G. Dongxin, Q. Guoqing, C. Guodong, & L. Shude]. *Arctic, Antarctic, and Alpine Research*, 33(2), 245–246. doi:10.2307/1552227.
- [2] Qiao, J., Zhen, J., Liu, Z. (2019). The distribution and major engineering problems of special soil and rock along One Belt One Road. *Journal of Catastrophology*, 65–71. doi:10.3969/j.issn.1000-811X.2019.Z1.012.
- [3] Cheng, G., Wu, Q., & Ma, W. (2009). Innovative designs of permafrost roadbed for the Qinghai-Tibet Railway. *Science in China, Series E: Technological Sciences*, 52(2), 530–538. doi:10.1007/s11431-008-0291-6.
- [4] Zhang, M., Pei, W., Li, S., Lu, J., & Jin, L. (2017). Experimental and numerical analyses of the thermo-mechanical stability of an embankment with shady and sunny slopes in permafrost regions. *Applied Thermal Engineering*, 127, 1478–1487. doi:10.1016/j.applthermaleng.2017.08.074.
- [5] Qi-Dong, D., Shao-Ping, C., Ji, M., & Peng, D. (2014). Seismic Activities and Earthquake Potential in the Tibetan Plateau. *Chinese Journal of Geophysics*, 57(5), 678–697. doi:10.1002/cjg2.20133.
- [6] Xi-yin, Z. H. A. N. G., Xing-chong, C. H. E. N., & Jian-qiang, G. A. O. Research advance on seismic performance of bridges in permafrost regions. *Journal of Lanzhou University of Technology*, 46(2), 116. (In Chinese).
- [7] Wanping, W. A. N. G., ZHANG, X., Xingchong, C. H. E. N., Yi, W. A. N. G., & Shengsheng, Y. U. Study on dynamic interaction between bridge pile and soil with permafrost effect: status and review. *Journal of Glaciology and Geocryology*, 4, 1213-1219.
- [8] Vali, R. (2021). Water Table Effects on the Behaviors of the Reinforced Marine Soil-footing System. *Journal of Human, Earth, and Future*, 2(3), 296–305. doi:10.28991/hef-2021-02-03-09.

- [9] Jin, H. J. (2006). Degradation of permafrost in the Da and Xiao Hinggan Mountains, Northeast China, and preliminary assessment of its trend. *Journal of Glaciology and Geocryology*, 28(4), 467-476.
- [10] Li, T., Wei, Q. C., & Liu, L. (2005). Effect of climate getting warmer on the seismic safety performance of Qinghai Tibet Railway bridges in the perennial frozen soil region. *Journal of the China Railway Society*, 27(4), 104-109.
- [11] Xiong, Z. H., Chen, J. B., Zhu, D. P. & Fu, J. (2018). Review of Design Method and Experiment on Bridge Pile Foundation in Permafrost Regions. *Low Temperature Architecture Technology*, 84–87. doi:10.13905/j.cnki.dwjz.2018.08.026.
- [12] Lai, Y. M., Zhang, Y., Zhang, S. J., Jin, L., & Chang, X. X. (2009). Experimental study of strength of frozen sandy soil under different water contents and temperatures. *Rock and Soil Mechanics*, 30(12), 3665–3670. doi:10.16285/j.rsm.2009.12.018.
- [13] Ekeleme, A. C., Ekwueme, B. N., & Agunwamba, J. C. (2021). Modeling Contaminant Transport of Nitrate in Soil Column. *Emerging Science Journal*, 5(4), 471–485. doi:10.28991/esj-2021-01290.
- [14] Aksenov, V. I., & Kistanov, O. G. (2008). Estimation of resistance components to an axial load on piles embedded in permafrost. *Soil Mechanics and Foundation Engineering*, 45(2), 71–75. doi:10.1007/s11204-008-9001-4.
- [15] Zhang, J., Zhang, Z., Zhang, S., Brouchkov, A., Xie, C., & Zhu, S. (2022). Numerical simulation of the influence of pile geometry on the heat transfer process of foundation soil in permafrost regions. *Case Studies in Thermal Engineering*, 102324. doi:10.1016/j.csite.2022.102324.
- [16] Jia, X. Y., Li, W. J., & Zhu, Y. Q. (2003). Analysis on hydration influence of grouting pile concrete in permafrost regions. *Journal of Shijiazhuang Railway Institute*, 16(4), 88-90. doi:10.13319/j.cnki.sjztdxxbzb.2003.04.023.
- [17] Hou, X., Chen, J., Jin, H., Rui, P., Zhao, J., & Mei, Q. (2020). Thermal characteristics of cast-in-place pile foundations in warm permafrost at Beiluhe on interior Qinghai-Tibet Plateau: Field observations and numerical simulations. *Soils and Foundations*, 60(1), 90–102. doi:10.1016/j.sandf.2020.01.008.
- [18] Chen, K., Yu, Q., Guo, L., Zhang, G., & Zhang, D. (2020). A fast-freezing system to enhance the freezing force of cast-in-place pile quickly in permafrost regions. *Cold Regions Science and Technology*, 179, 103140. doi:10.1016/j.coldregions.2020.103140.
- [19] Shang, Y., Niu, F., Lin, Z., & Sun, T. (2020). Analysis of the cooling effect of a concrete thermal pile in permafrost regions. *Applied Thermal Engineering*, 173, 115254. doi:10.1016/j.applthermaleng.2020.115254.
- [20] Shang, Y., Niu, F., Wu, X., & Liu, M. (2018). A novel refrigerant system to reduce refreezing time of cast-in-place pile foundation in permafrost regions. *Applied Thermal Engineering*, 128, 1151–1158. doi:10.1016/j.applthermaleng.2017.09.079.
- [21] Yan, N., & Yu, T. (2020). Heat Transfer between Concrete Bored Cast-In-Place Piles and Surrounding Frozen Soil in Ice-Rich Area. *Journal of Civil, Construction and Environmental Engineering*, 5(5), 102. doi:10.11648/j.jccee.20200505.11.
- [22] Hou, X., Chen, J., Yang, B., Wang, J., Dong, T., Rui, P., & Mei, Q. (2022). Monitoring and simulation of the thermal behavior of cast-in-place pile group foundations in permafrost regions. *Cold Regions Science and Technology*, 196, 103486. doi:10.1016/j.coldregions.2022.103486.
- [23] Chen, J. B., Li, J. P., & Xiong, Z. H. Inspection of Bridge Damage in Maduo Earthquake and Its Effects on Bridge Design in Cold Region. *Journal of Water Resources and Architectural Engineering*, 19(05), 99–104. doi:10.3969/j.issn.1672-1144.2021.05.018. (In Chinese).
- [24] Teng, J. (2018). New-material hybrid structures. *Tumu Gongcheng Xuebao/China Civil Engineering Journal*, 51(12), 1–11. (In Chinese)
- [25] Ziehl, P. H., Engelhardt, M. D., Fowler, T. J., Ulloa, F. V., Medlock, R. D., & Schell, E. (2009). Design and Field Evaluation of Hybrid FRP/Reinforced Concrete Superstructure System. *Journal of Bridge Engineering*, 14(5), 309–318. doi:10.1061/(asce)be.1943-5592.0000002.
- [26] Petzek, E., & Bancila, R. (2010). Efficient solutions for composite bridges. *International Scientific Conference. CIBv2010. 12 – 13 November 2010, Braşov, Romania*.
- [27] Xiong, Z., Li, J., Wang, S., Liu, Y., & Xin, H. (2018). Concrete filled tubular arch modified-VFT bridge and its LLSI analysis. *Proceedings of the 2017 3rd International Forum on Energy, Environment Science and Materials (IFEESM 2017)*. doi:10.2991/ifeesm-17.2018.250.
- [28] Xiong, Z., Li, J., Zhu, H., Liu, X., & Liang, Z. (2022). Ultimate Bending Strength Evaluation of MVFT Composite Girder by using Finite Element Method and Machine Learning Regressors. *Latin American Journal of Solids and Structures*, 19(3). doi:10.1590/1679-78257006.
- [29] Xiong, Z. H., Chen, J. B., & Wang, S. S. Structural analysis of prefabricated steel-concrete composite bridge applied in cold and high-altitude permafrost regions. *Steel Construction*, 33(04), 46-51. (In Chinese).
- [30] China Communications Construction Company Ltd. (2017). Highway construction technology in high altitude and cold regions. CCCC First Highway Consultants Co. China. Available online: <http://en.ccccltd.cn/> (accessed on May 2022).

- [31] JTG 3363-2019. (2019). Specifications for Design of Foundation of Highway Bridges and Culverts. Specification for design of Foundation of Highway Bridge and Culverts, Ministry of Transport of the People's Republic of China, Beijing, China. Available online: <https://m.freebz.net/hangye/299522.html> (accessed on May 2022).
- [32] Yanmin, J., Da, X., & Hongyu, G. (2010). Study on phase transformation effect due to refrozen process of cast-in-place piles and frozen soil. *Engineering Mechanics*, 27(Suppl 1), 144-149. (In Chinese).
- [33] Xiong, W., Liu, M. G., Zhang, Q. H., & Wang, Z. M. (2009). Temperature distribution along piles in permafrost regions. *Yantu Lixue / Rock and Soil Mechanics*, 30(6), 1658–1664. doi:10.16285/j.rsm.2009.06.009.
- [34] Shang, Y.-H. Study on ground temperature of cast-in-place pile of bridge in permafrost regions. *Journal of Glaciology and Geocryology*, 38(4), 1129–1135. doi:10.7522/j.issn.1000-0240.2016.0131.
- [35] Peng, X., Lan, C., Wang, S., Sui, S., & Zeng, L. (2015). Effects of the C-S-H powder on the hydration process and mechanism of cement. *Jianzhu Cailiao Xuebao/Journal of Building Materials*, 18(2), 195–201. doi:10.3969/j.issn.1007-9629.2015.02.003. (In Chinese).
- [36] He, R. X., Jin, H. J., Zhao, S. P., & Deng, Y. S. (2018). Review of status and progress of the study in thermal conductivity of frozen soil. *Journal of Glaciology Geocryology*, 40(1), 116–126. doi:10.7522/j.issn.1000-0240.2017.0314. (In Chinese).